Journal of Bacteriology

Characterization of CrgA, a New Partner of the Mycobacterium tuberculosis Peptidoglycan Polymerization Complexes

P. Plocinski, M. Ziolkiewicz, M. Kiran, S. I. Vadrevu, H. B. Nguyen, J. Hugonnet, C. Veckerle, M. Arthur, J. Dziadek, T. A. Cross, M. Madiraju and M. Rajagopalan

J. Bacteriol. **2011, 193(13):3246. DOI: 10.1128/JB.00188-11.**
Published Ahead of Print 29 April 2011.

Updated information and services can be found at:
http://jb.asm.org/content/193/13/3246

These include:

SUPPLEMENTAL MATERIAL http://jb.asm.org/content/suppl/2011/06/09/193.13.3246.DC1.html

REFERENCES This article cites 53 articles, 31 of which can be accessed free at: http://jb.asm.org/content/193/13/3246#ref-list-1

CONTENT ALERTS Receive: RSS Feeds, eTOCs, free email alerts (when new articles cite this article), more»

Information about commercial reprint orders: **http://jb.asm.org/site/misc/reprints.xhtml**
To subscribe to to another ASM Journal go to: **http://journals.asm.org/site/subscriptions/**

Journals.ASM.org

Downloaded from http://jb.asm.org/ on January 31, 2012 by FLORIDA STATE UNIV

JOURNAL OF BACTERIOLOGY, July 2011, p. 3246–3256 Vol. 193, No. 13
0021-9193/11/$12.00 doi:10.1128/JB.00188-11
Copyright © 2011, American Society for Microbiology. All Rights Reserved.

Characterization of CrgA, a New Partner of the *Mycobacterium tuberculosis* Peptidoglycan Polymerization Complexes▽†

P. Plocinski,[1] M. Ziolkiewicz,[2] M. Kiran,[1] S. I. Vadrevu,[1] H. B. Nguyen,[3]‡ J. Hugonnet,[4] C. Veckerle,[4] M. Arthur,[4] J. Dziadek,[2] T. A. Cross,[3] M. Madiraju,[1] and M. Rajagopalan[1]*

The University of Texas Health Science Center at Tyler, Biomedical Research, Tyler, Texas 75708[1]; Polish Academy of Sciences, Lodz, Poland[2]; The National High Magnetic Field Lab and the Department of Chemistry and Biochemistry, Florida State University, Tallahassee, Florida 32306[3]; and Centre de Recherche des Cordeliers, INSERM UPMC UPD, Université Pierre et Marie Curie, 15 rue de l'Ecole de Médecine, Paris, Cedex, France[4]

Received 10 February 2011/Accepted 20 April 2011

The role(s) in cell division of the *Mycobacterium tuberculosis* Rv0011c gene product, a homolog of the *Streptomyces* CrgA protein that is responsible for coordinating growth and cytokinesis in sporogenic aerial hyphae, is largely unknown. We show that an enhanced cyan fluorescent protein-*M. tuberculosis* CrgA (ECFP-$CrgA_{MT}$) fusion protein is localized to the cell membrane, midcell, and cell pole regions in *Mycobacterium smegmatis*. Furthermore, the ECFP-$CrgA_{MT}$ fusion protein colocalized with FtsZ-enhanced yellow fluorescent protein (EYFP) in *M. smegmatis*. Bacterial two-hybrid assays indicated strong interactions of *M. tuberculosis* CrgA with FtsZ, FtsQ, and the class B penicillin-binding proteins, FtsI (PBPB) and PBPA. The midcell localization of $CrgA_{MT}$ was severely compromised under conditions of FtsZ depletion, which indicated that CrgA localizes to the midcell region after assembly of the FtsZ ring. *M. tuberculosis* cells with reduced CrgA levels were elongated and grew more slowly than wild-type cells, which indicated defects in cell division, whereas CrgA overproduction did not show growth defects. A *M. smegmatis* Δ*crgA* strain exhibited a bulged cell morphology, elongated cells with a chain-like phenotype, cells with polar bulbous structures, and a modest growth defect. FtsZ and FtsI levels were not affected in cells producing altered levels of CrgA. Septal and membrane localization of GFP-FtsI was enhanced by CrgA overproduction and was diminished in a Δ*crgA* strain, which indicates that one role of CrgA is to promote and/or stabilize FtsI localization. Overall, these data indicate that CrgA is a novel member of the cell division complex in mycobacteria and possibly facilitates septum formation.

Mycobacterium tuberculosis is the causative agent of tuberculosis. Tuberculosis remains a leading cause of worldwide morbidity and mortality. The recent emergence of extensively drug-resistant strains of *M. tuberculosis* and the widespread development of multidrug-resistant strains have once again underscored the importance of developing new antimycobacterial agents (3). Pathways essential for bacterial survival represent good targets for drug development. DNA replication and cell division are two such pathways essential for bacterial multiplication and, therefore, survival (39).

Assembly of the cell division initiator FtsZ as distinct structures at midcell sites, referred to as FtsZ rings (Z-rings), is the first step in the initiation of cell division in almost all eubacteria. The FtsZ ring then serves as a scaffold for recruitment of other divisome proteins (2). Recent studies implicate a role for FtsZ in guiding septum and lateral cell wall synthesis in some bacterial species (1, 48). FtsZ interacts with a number of proteins during various cell division steps, and FtsZ assembly is subject to positive and negative regulation. FtsA, a widely conserved FtsZ-interacting protein, is membrane tethered and required for the assembly of the FtsZ ring and for the recruitment of downstream proteins (10, 40). ZipA, another FtsZ-interacting protein present in *Gammaproteobacteria*, is also a membrane-anchored protein that promotes FtsZ ring assembly (26, 41). ZapA is a positive regulator of FtsZ ring assembly and stability, and SepF is required for proper septum formation (24, 28, 32). ZapB is a novel factor that concurrently stimulates FtsZ ring assembly and cell division (21). SulA is a DNA damage-inducible cell division inhibitor that promotes FtsZ disassembly (36, 46). *Bacillus subtilis* EzrA regulates FtsZ assembly dynamics and coordinates cell elongation with cell division (8, 35). MciZ is a 40-amino-acid (aa) peptide involved in the inhibition of FtsZ ring assembly following sporulation in *B. subtilis* (29). ClpX, a part of the ClpXP protease complex, inhibits FtsZ polymerization and possibly helps to maintain cytoplasmic pools of unpolymerized FtsZ subunits (5, 20, 25, 44, 50). Finally, the Min system spatially regulates cell division by preventing FtsZ assembly at the cell poles (27). More recently, MinC has been shown to regulate cell division by affecting the scaffolding function of FtsZ (11).

CrgA, a member of a novel family of small proteins present in actinomycetes, was first described in *Streptomyces* species, where it was shown to affect sporulation septation and influence FtsZ ring assembly by affecting FtsZ protein turnover (15, 16). Specifically, growth of a *Streptomyces coelicolor* Δ*crgA*

* Corresponding author. Mailing address: The University of Texas Health Science Center at Tyler, Biomedical Research, Tyler, Texas 75708. Phone: (903) 877-7731. Fax: (903) 877-5969. E-mail: malini.rajagopalan@uthct.edu.

‡ Present address: Bioscience Division, Los Alamos National Laboratory, Los Alamos, New Mexico 87545.

† Supplemental material for this article may be found at http://jb.asm.org/.

▽ Published ahead of print on 29 April 2011.

Downloaded from http://jb.asm.org/ on January 31, 2012 by FLORIDA STATE UNIV

strain on glucose-containing medium results in premature development of aerial hyphae, formation of spores with abnormal swollen morphology, early antibiotic production, and a 3- to 4-fold increase in the abundance of FtsZ rings (16). Overproduction of CrgA inhibits FtsZ ring formation and promotes proteolytic turnover of FtsZ and growth of nonseptate hyphae in *S. coelicolor* (15). On the other hand, *crgA* is required for sporulation septum formation in aerial hyphae of *Streptomyces avermitilis* (16). Homologs of CrgA are present in other actinomycetes, such as *Corynebacterium* and *Mycobacterium* species, including *Mycobacterium leprae*. The mycobacterial CrgA homolog has not been characterized.

Although cell division machinery is generally well conserved in eubacteria, mycobacteria lack genes encoding several well-characterized regulatory proteins, e.g., EzrA, ZapA, ZapB, SulA, and MinCDE, and also some integral components, e.g., FtsA, FtsN, and FtsB (30). Despite this fact, the slow polymerization and weak GTP hydrolysis activities of *M. tuberculosis* FtsZ combined with the presence of novel proteins such as ChiZ and FipA, which indirectly or directly modulate FtsZ ring assembly, impart uniqueness to the mycobacterial cell division machinery (6, 7, 45, 52). Interaction of FtsZ with phosphorylated FipA is thought to be necessary for productive cell division under oxidative stress (45). ChiZ, an *M. tuberculosis* cell wall hydrolase, is induced upon DNA damage and regulates midcell FtsZ assembly (7). *M. tuberculosis* FtsZ interacts with FtsW, and this interaction is implicated in providing stability to the FtsZ ring (13, 42). Presumably, novel pathways are also involved in the regulation of *M. tuberculosis* cell division and cell wall synthesis.

In this work, we examined the role of mycobacterial CrgA in cell division. Our studies indicate that CrgA is an abundant protein that interacts with FtsZ, FtsI, the penicillin-binding protein PBPA, and FtsQ and localizes to the midcell region in a FtsZ-dependent manner. CrgA overproduction altered the cellular localization of green fluorescent protein (GFP)-FtsI. Deletion of *crgA* in *Mycobacterium smegmatis* ($crgA_{MS}$) slowed the growth rate and led to defects in septum splitting and to the formation of bulged cells. Our results suggest that CrgA is a component of the mycobacterial cell division machinery that plays an important role in septal peptidoglycan (PG) synthesis and cell shape morphogenesis.

MATERIALS AND METHODS

Bacterial strains and growth conditions. The bacterial strains used in this study are listed in Table 1. *E. coli* strain Top10 was used for cloning purposes and propagated in Luria-Bertani (LB) broth. Transformants were selected on LB agar containing either ampicillin (Amp; 100 μg/ml), kanamycin (Km; 50 μg/ml), or hygromycin (Hyg; 200 μg/ml). *M. smegmatis* mc^2155 and *M. tuberculosis* H37Rv were grown in Middlebrook 7H9 broth supplemented with albumin-dextrose (AD) and oleic acid, albumin, dextrose, and sodium chloride, respectively. Transformants were selected in this same medium supplemented with agar containing either Km (10 μg/ml), Hyg (50 μg/ml), or both. When required, acetamide and/or anhydrotetracycline was supplied in the growth medium at a final concentration of 0.2% acetamide and 10 to 100 ng/ml anhydrotetracycline (19, 20). Growth was followed by monitoring absorbance at 600 nm.

PCR and gene cloning methods. PCR fragments were generated using Phusion or Deep Vent DNA polymerase and cloned into the appropriate vectors. The coding regions of *crgA*, *ftsZ*, *pbpA*, and *pbpB* or their derivatives encoding fluorescent fusion proteins (*ftsZ-gfp*, *ftsZ-yfp*, *gfp-crgA*, *ecfp-crgA*, *gfp-pbpA*, and *gfp-pbpB*) were expressed from acetamide (*Pami*)- or tetracycline-inducible (*Ptet*) promoters. For bacterial two-hybrid (BACTH) constructs, the coding regions of various genes were cloned in frame into four vectors as previously described (34). All cloned fragments were confirmed by sequencing. For protein purification, *crgA* was cloned into pET29b and pMAL-c4E vectors, whereas *ftsZ* and *clpX* were cloned into pET19b and pMAL-c4e, respectively (Table 1).

Construction of an *M. smegmatis crgA* knockout strain. A *crgA* mutant strain was constructed using a suicide plasmid, pPP107 (Table 1) and a two-step recombination protocol (38). Briefly, a 996-bp BamHI-HindIII fragment containing the *crgA* coding region, together with the upstream 398-bp and the downstream 314-bp regions, was cloned into pMAL-c4E (Table 1, pPP102a). Next, the *crgA* gene was interrupted by blunt-end cloning an 850-bp gentamicin cassette into the XmnI site 27 bp from the N-terminal end of *crgA* (Table 1, pPP102). The insertion led to disruption of the *crgA* reading frame. The ~1,800-bp BamHI-HindIII fragment was subsequently subcloned in the same sites of the p2NIL suicide vector (38) (Table 1, pPP103). Finally, a 6.1-kb PacI fragment carrying the *lacZ*, *aph*, and *sacB* genes was inserted into pPP103 to create the recombination suicide plasmid, pPP107 (Table 1). This plasmid was electroporated into *M. smegmatis* to replace *crgA* at the native locus by homologous recombination.

Microscopy. Wild-type (WT) and recombinant *M. tuberculosis* strains were grown for various periods of time with shaking and were then harvested by centrifugation, washed in phosphate-buffered saline (PBS), fixed in 4% paraformaldehyde, and stored at 4°C until further use. GFP-CrgA, enhanced cyan fluorescent protein (ECFP)-CrgA, GFP-PBPB, and GFP-PBPA localization could not be visualized in *M. tuberculosis* due to fluorescence bleaching, which was caused by the paraformaldehyde fixation required for this virulent strain (20). Therefore, all the cellular localization experiments were carried out in the nonpathogenic *M. smegmatis* mc^2155 strain. Cell division proteins in various mycobacterial species have shown a high degree of homology, and *M. smegmatis* has therefore served as a favorite surrogate host for cell division protein localization studies (6, 14, 19, 20, 33). Bocillin-FL, a fluorescent derivative of penicillin V, was used to visualize the overall localization of penicillin-binding proteins in *M. smegmatis* strains expressing altered CrgA levels. Briefly, actively growing cultures of *M. smegmatis* recombinant strains were induced with 100 ng/ml anhydrotetracycline, and 1 μg/ml Bocillin-FL was then added to the cultures for 2 h. Plasma membranes, including newly formed cell division septa, were visualized by staining with FM4-64 [*N*-(3-triethylammoniumpropyl)-4-(6-(4-(diethylamino)phenyl) hexatrienyl) pyridinium dibromide], a styryl lipophilic dye. Exponential-phase cultures were grown with 0.1 μg/ml of FM4-64 for various time periods, and cells were examined by fluorescence microscopy. A Nikon Eclipse 600 microscope equipped with a 100× Nikon Plan Fluor oil immersion objective with a numerical aperture of 1.4 and appropriate filter sets (Chroma) were used for bright-field and fluorescence microscopy. Images were acquired using a Photometrics Coolsnap ES camera and Metapmorph, version 6.2, imaging software (Universal Imaging Corporation). Images were optimized using Adobe Photoshop CS4.

Protein-protein interaction experiments. (i) BACTH assay. A BACTH system kit (Euromedex) was used to investigate CrgA interactions with other cell division proteins as previously described (20). *Escherichia coli* BTH101 recombinants containing various combinations of plasmids (Table 1) were selected on LB agar supplemented with 40 μg/ml 5-bromo-4-chloro-3-indolyl-β-D-galactopyranoside. (X-Gal), 0.5 mM isopropyl-β-D-thiogalactopyranoside (IPTG), and antibiotics. Strength of interaction, indicated by the extent of β-galactosidase activity, was measured using cultures grown in LB medium. β-Galactosidase-specific activity is defined as units/mg of dry weight bacteria, and 1 unit corresponds to 1 nmol of *o*-nitrophenyl-β-D-galactopyranoside (ONPG) hydrolyzed per min at 28°C. β-Galactosidase activity 5-fold higher than that of the BTH101 control, which carried a single copy of the gene and an empty vector, was considered indicative of an interaction. *E. coli* BTH101 transformants obtained with pKT25-GCN4 and pUT18C-GCN4 (harboring the *Bordetella pertussis* adenylate cyclase T25 and T18 subdomains, respectively) served as positive controls for complementation (Table 1).

(ii) Pulldown assay. A Pierce His Protein Interaction Pull-down kit (Pierce) was used to examine the CrgA-FtsZ interaction. Briefly, lysates of *E. coli* cells expressing the proteins or purified proteins were mixed with a Profound lysis buffer–Tris-buffered saline (TBS) mixture (1:1) and incubated on ice for 30 min with gentle mixing. The protein mixture was then incubated with preequilibrated cobalt affinity resin for 1 h (4°C) with gentle rocking, and the resin-protein mixture was loaded into a spin column. The flowthrough was collected. The affinity resin was washed seven times with 0.5-ml volumes of the lysis buffer-TBS mixture (1:1), and bound proteins were eluted with the same buffer supplemented with 300 mM imidazole. Eluted proteins were subsequently visualized by SDS-PAGE electrophoresis followed by immunoblotting.

Immunoblotting. FtsZ, FtsI, and CrgA proteins in *M. tuberculosis* ($FtsZ_{MT}$, $FtsI_{MT}$, and $CrgA_{MT}$, respectively) and/or *M. smegmatis* wild-type and *crgA*

Downloaded from http://jb.asm.org/ on January 31, 2012 by FLORIDA STATE UNIV

TABLE 1. Strains and plasmids

Strain or plasmid	Description	Reference or source
Strains		
E. coli Top10 F′		Invitrogen, Inc.
E. coli C41(DE3)		Avidis SA, France
M. tuberculosis H37Rv		Lab stock
M. smegmatis mc^2155		Lab stock
M. smegmatis FZ-3	FtsZ conditional expression strain	19
Plasmids		
pMV306	Integration proficient *E. coli-Mycobacterium* shuttle vector; Km^r	43
p2NIL	Suicide recombination vector; Km^r	38
pGOAL17	Carrying 6.1-kb PacI cassette; Km^r	38
pDS5	$crgA_{MT}$ cloned in pLR52 vector; Hyg^r	This study
pET-19b	*E. coli* expression vector allowing fusions to N-terminal His_6 tag; Amp^r	Novagen
pRSF-Duet	*E. coli* expression vector allowing fusions to N-terminal His_6 or C-terminal S tag; Km^r	Novagen
pMAL-c4E	*E. coli* expression vector allowing fusions with N-terminal MBP; Amp^r	NE Biolabs
pET29b	*E. coli* expression vector; Km^r	Novagen
pMK10	Antisense $crgA_{MT}$ sequence (1 to 282-bp antisense coding strand) cloned in pLR56 vector; Km^r	This study
pHN-CrgA	$crgA_{MT}$ coding sequence cloned in pET29b; Km^r	This study
pJFR79	FtsZ-GFP cloned in pJAM2; Km^r	19
pPP30	$crgA_{MT}$-*ecfp* cloned in pLR52 vector; Hyg^r	This study
pSAR1	His_6-$ftsZ_{MT}$ cloned in pET19b; Amp^r	This study
pLR66	S-tagged $FtsZ_{MT}$ cloned in pRSF-Duet; Km^r	20
pMR121	$ftsZ_{MT}$-*eyfp* cloned in pMG103; Km^r	20
pKT25	*E. coli* expression vector allowing fusions to the C terminus of the T25 fragment of *cyaA*; Km^r	34
pUT18C	*E. coli* expression vector allowing fusions to the C terminus of the T18 fragment of *cyaA*; Amp^r	34
pKNT25	*E. coli* expression vector allowing fusions to the N terminus of the T25 fragment of *cyaA*; Km^r	34
pUT18	*E. coli* expression vector allowing fusions to N terminus of the T18 fragment of *cyaA*; Amp^r	34
pPP48	$crgA_{MT}$ cloned in pUT18C vector; Amp^r	This study
pPP51	$pbpA_{MT}$ cloned in pUT18C; Amp^r	This study
pPP52	$pbpA_{MT}$ cloned in pKT25; Km^r	This study
pPP53	$crgA_{MT}$ cloned in pKT25 vector; Km^r	This study
pPP54	$rodA_{MT}$ cloned in pUT18C; Amp^r	This study
pPP55	$rodA_{MT}$ cloned in pKT25; Km^r	This study
pPP56	$clpX_{MT}$ cloned in pKT25; Km^r	This study
pPP57	$clpX_{MT}$ cloned in pUT18; Amp^r	This study
pMK18	$ftsI_{MT}$ cloned in pUT18C; Amp^r	20
pMK19	$ftsI_{MT}$ cloned in pKT25; Km^r	20
pMK20	$ftsQ_{MT}$ cloned in pUT18C; Amp^r	20
pMK21	$ftsQ_{MT}$ cloned in pKT25; Km^r	20
pMK23	$clpX_{MT}$ cloned in pMALc-4E; Amp^r	20
pPP79	*gfp*-$ftsI_{MT}$ cloned into pMG103 vector; Km^r	This study
pPP82	$crgA_{MT}$ cloned into pMAL-c4e vector; Amp^r	This study
pPP88	$crgA_{MT}$ cloned into pRSF-Duet; Km^r	This study
pPP91	ECFP-$CrgA_{MT}$ with a deletion of the C terminus cloned into pLR52; Hyg^r	This study
pPP93	ECFP-$CrgA_{MT}$ with a deletion of the N terminus cloned into pLR52; Hyg^r	This study
pPP94	Amino acids 1 to 124 of $FtsI_{MT}$ cloned into pUT18C; Amp^r	This study
pPP96	Amino acids 1 to 298 of $FtsI_{MT}$ cloned into pUT18C; Amp^r	This study
pPP102a	996-bp *crgA* region containing the *crgA* coding region with upstream 398 bp and downstream 314 bp cloned into pMAL-c4E; Amp^r	This study
pPP102	*crgA* coding region in pPP102a interrupted with 850-bp gentamicin cassette insertion; Amp^r	This study
pPP103	~1,800-bp BamHI-HindIII fragment from pPP102 in p2NIL; Km^r	This study
pPP107	pPP103 with 6.1-kb PacI cassette from pGOAL17; Km^r Suc^r *lacZ*	This study
pPP110	Amino acids 1 to 51 of $CrgA_{MT}$ cloned into pKT25; Km^r	This study
pPP111	Amino acids 1 to 51 of $CrgA_{MT}$ cloned into pUT18; Amp^r	This study
pPP113	Amino acids 1 to 51 of $CrgA_{MT}$ cloned into pMAL-c4E; Amp^r	This study
pPP119	*msmeg0026* under the control of the native promoter cloned into pMV306; Km^r	This study
pLR56	*Mycobacterium* integrating vector, with *tet* promoter and *tet* repressor; Hyg^r	20
pLR52	*E. coli-Mycobacterium* shuttle vector, replicating, with *tet* promoter and *tet* repressor; Hyg^r	20

Downloaded from http://jb.asm.org/ on January 31, 2012 by FLORIDA STATE UNIV

strains were detected by immunoblotting as previously described (19). Cell lysates were prepared from exponentially grown cultures (20). Anti-SigA was used as a loading control since SigA levels do not change during growth (7). Blots were probed simultaneously with anti-$FtsZ_{MT}$ and anti-$SigA_{MT}$ antibodies. Pulldown assay fractions were also visualized by immunoblotting using anti-CrgA, anti-FtsZ, or anti-MBP antibodies as needed. Immunoblots were processed using an ECF Western blotting kit (GE Life Sciences; Piscataway, NJ) and scanned using a Bio-Rad Molecular Imager (FX). Protein levels were determined using the volume analysis function of QuantityOne software. The CrgA levels in *M. tuberculosis* were determined using a standard curve prepared with pure protein as previously described (see supplemental material).

CrgA purification. $crgA_{MT}$ was expressed with a noncleavable C-terminal His tag from pET29b (EMD Chemicals) in *E. coli* strain BL-21(DE3) CodonPlus-RP (Agilent Technologies) or as a maltose-binding protein (MBP)-CrgA fusion in pMAL-c4E (New England Biolabs) in *E. coli* strain C41(DE3). Both strains were grown in LB broth to an optical density at 600 nm (OD_{600}) of 0.6 to 0.8 and induced with 1 mM IPTG. CrgA-His cells were lysed by sonication in a buffer containing 40 mM Tris-HCl (pH 8.0), 300 mM NaCl, 1.1 mM phenylmethylsulfonyl fluoride (PMSF), 0.02 mg/ml benzonase (EMD Chemicals), and 0.2 mg/ml lysozyme. After solubilization with 3% Empigen for 1 h, lysates were centrifuged, and supernatants containing CrgA-His were loaded onto a nickel-nitrilotriacetic acid (Ni-NTA) resin column. The column was washed with 40 mM Tris-HCl (pH 8.0), 300 mM NaCl, 30 mM imidazole, and 2 mM dodecylphosphocholine (DPC; Anatrace, Inc.). Bound proteins were eluted in the same buffer containing 250 mM imidazole and 0.2% DPC. For MBP-CrgA purification, cells were harvested as described above and lysed by sonication in MBP column buffer (20 mM Tris-HCl [pH 7.4], 200 mM NaCl, 1 mM EDTA, 0.5% 3-[(3-cholamidopropyl)-dimethylammonio]-1-propanesulfonate [CHAPS], and 1% NP-40 detergent). MBP-CrgA was purified according to the manufacturer's protocol (NEB, MA). Peak fractions were pooled and passed through a hydroxyapatite column to remove maltose. MBP-CrgA was finally eluted into sodium phosphate buffer (pH 7.4) supplemented with 0.5% CHAPS and 1% NP-40 detergent. The protein was dialyzed against 25 mM Tris-HCl (pH 7.2), 150 mM NaCl, and 10% glycerol. When required, the MBP tag was removed following cleavage with enterokinase using the manufacturer's protocol (NEB). A C-terminal truncation of $CrgA_{MT}$ consisting of amino acids 1 to 51 was expressed as an MBP fusion protein in pMAL-c4E in *E. coli* strain C41(DE3) and purified following essentially the protocol used for the full-length protein.

RESULTS

CrgA is an abundant protein in *M. tuberculosis*. *M. tuberculosis* CrgA, like its *Streptomyces* homolog, is a small membrane protein with two transmembrane regions. Each region is composed of 25 amino acids linked by a 14-amino-acid extracytoplasmic loop. The N-terminal cytoplasmic end is comprised of 26 amino acids, and the C-terminal tail is only 3 amino acids long (15, 16). To examine the role of a CrgA-like protein in *M. tuberculosis*, we first determined if the homolog encoded by Rv0011c is, indeed, expressed in *M. tuberculosis*. Immunoblotting using antibodies specific to the N-terminal end of CrgA indicated the presence of an ~11-kDa protein (see Fig. S1, bottom panel, in the supplemental material). Comparative quantitation of the specific band against purified CrgA led to the determination that CrgA levels in exponential cultures of *M. tuberculosis* were ~20,000 molecules per cell (see Fig. S1). These results suggested that CrgA is nearly as abundant as FtsZ and MtrA (18, 22).

Altered CrgA levels affect *M. tuberculosis* cell morphology. To determine the role(s) of CrgA in cell division, we constructed *M. tuberculosis* strains expressing elevated (sense strain) or decreased (antisense strain) levels of CrgA (Table 1). Addition of the inducer, anhydrotetracycline, for 48 h increased CrgA levels ~5-fold in the sense strain, whereas the protein was reduced by approximately 33% in the antisense strain (Fig. 1A, inset). CrgA overproduction did not significantly affect cell growth or morphology, but a reduction in the

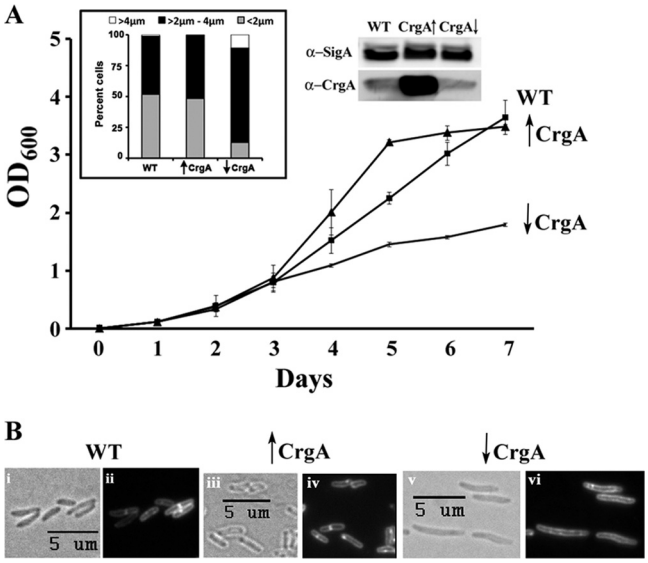

FIG. 1. Alteration in CrgA levels affects growth and cell division of *M. tuberculosis*. Wild-type, overexpression (↑), and antisense (↓) *crgA* strains of *M. tuberculosis* were grown with 100 ng/ml anhydrotetracycline, and growth was monitored and plotted (A). Levels of CrgA were examined by immunoblotting (inset). Cell length measurements for the three strains were made from at least 100 cells each, and data were plotted (inset). (B) At day 2 postinduction with anhydrotetracycline, bacteria were stained with membrane dye FM4-64 and examined by bright-field (i, iii, and v) and fluorescence (ii, iv, and vi) microscopy. α, anti.

synthesis of the protein decreased the growth rate (Fig. 1A) and increased the cell length from 2.20 ± 0.06 μm to 3.00 ± 0.05 μm (Fig. 1A, inset). Defects in cell division were also shown by the lack of septa following FM4-64 staining (Fig. 1B). Alterations in CrgA levels did not affect FtsZ levels (see Fig. S2, panel i, in the supplemental material).

An *M. smegmatis crgA* mutant strain shows defects in septum formation and cell shape. Although levels of CrgA were reduced by approximately only one-third, antisense *crgA* expression caused a growth defect and filamentation in *M. tuberculosis*. This raised the possibility that CrgA levels are important for the growth of *M. tuberculosis* and other mycobacteria. A CrgA homolog in the nonpathogenic *M. smegmatis* shows 94% similarity and 79% identity to the *M. tuberculosis* protein, which suggests functional conservation. Therefore, to further understand the role of CrgA in mycobacteria, we created an *M. smegmatis crgA* mutant strain by following a two-step homologous recombination protocol (Fig. 2A) (38). A gentamicin cassette was inserted 27 bp from the N-terminal end of the *crgA* coding region to disrupt the reading frame of the protein. Immunoblotting indicated the complete absence of CrgA in the mutant strain (see Fig. S3A in the supplemental material). The mutant strain showed a modest growth defect, with ~50% reduction in viability compared to the wild-type strain (Fig. 2B; also data not shown). The mutant cells were elongated and bulgy and sometimes grew with a chain-like phenotype (Fig. 2C). This phenotype suggested defects in septal constriction. Bulgy cells and chain-linked cells accounted for 41% and 16% in the mutant strain (n = 205) versus 7.5% and 4%, respectively, in the wild-type strain (n = 252). Septal staining with

Downloaded from http://jb.asm.org/ on January 31, 2012 by FLORIDA STATE UNIV

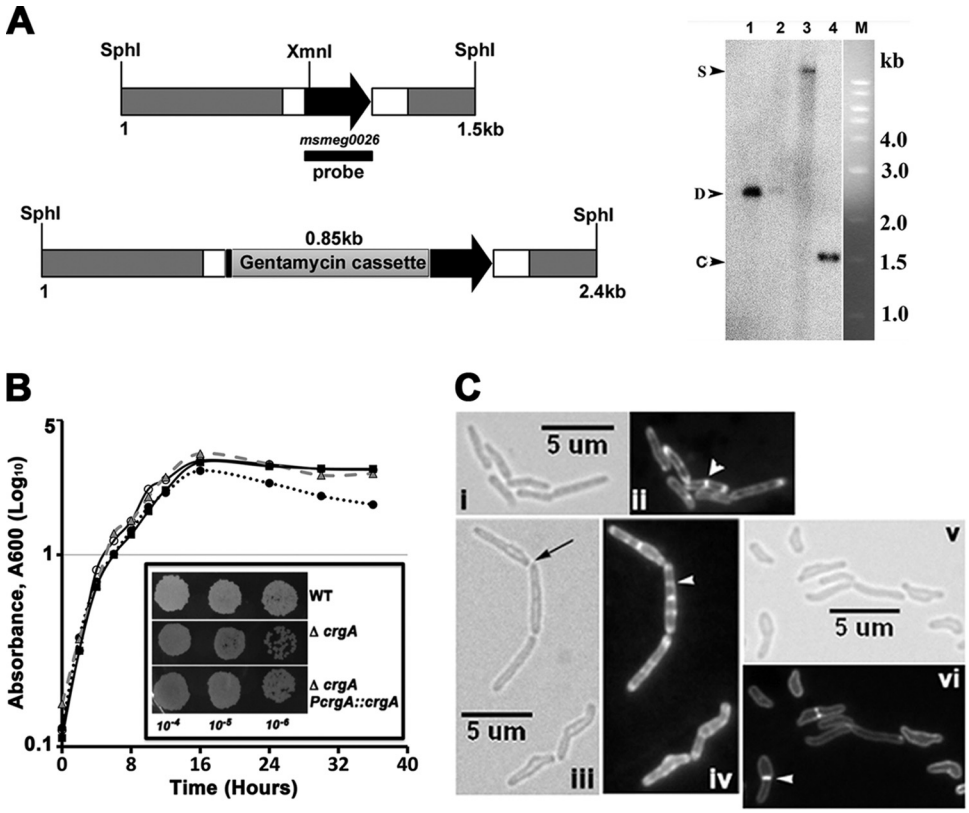

FIG. 2. Lack of CrgA affects cell division and cell shape. (A) Cartoon of the *crgA* (*msmeg0026*) region of *M. smegmatis* (top panel) with an inserted copy of the gentamicin cassette in p2NIL (Table 1, pPP107). Dark gray boxes, *crgA* flanking regions; light gray box, gentamicin cassette; black arrow, *crgA* coding region; white boxes, intergenic regions. At right is a Southern blot confirming replacement of *crgA* with a mutant copy. Genomic DNA was isolated from wild-type *M. smegmatis* mc^2155 (lane 4), single-crossover (lane 3), and two double-crossover (lanes 1 and 2) strains, digested with SphI restriction enzyme, transferred to nitrocellulose membrane, and probed with a ^{32}P-labeled *msmeg0026* fragment (probe in top panel). Positions of *msmeg0026* single-crossover (S), double-crossover (D), and chromosomal (C) copy bands are marked. Double-crossover 1 was further characterized with respect to growth and morphology. (B) Growth curve for *M. smegmatis* WT (open circles), Δ*crgA* strain (solid circles), and Δ*crgA PcrgA*::*crgA* (open triangles) and Δ*crgA Ptet*::*ecfp*::*crgA* (solid squares) complement strains. Overnight cultures of these strains were diluted to an A_{600} of 0.1 and grown in 7H9 broth supplemented with albumin and dextrose. Growth was followed by measuring A_{600} at the indicated time points, and data were plotted with Excel. The experiment was done three times, and one representative data set is shown. (Inset) Serial dilutions of exponential cultures of WT, Δ*crgA*, and Δ*crgA PcrgA*::*crgA* strains were prepared, and 10 μl was spotted on 7H9 medium-albumin-dextrose agar plates and grown at 37°C. (C) Morphology of *M. smegmatis crgA* mutant cells. The wild-type (i and ii) and mutant (iii to vi) strains were grown in 7H9 medium-albumin-dextrose broth, stained with FM4-64, and imaged by bright-field (i, iii, and v) and fluorescence (ii, iv, and vi) microscopy. Black arrow, incompletely split septa; white arrowhead, FM4-64-stained septa.

FM4-64 revealed that loss of CrgA led to a decrease in number of cells with one septum (Δ*crgA* strain, 19.5% [$n = 128$]; WT, 28.5% [$n = 147$]) and an increase in number of cells with 2 or more septa and cells with aberrantly placed septa (Δ*crgA* strain, 17.1%; WT, 4.4%). The growth and cell morphology defects were nearly reversed in the complemented strains that carried an integrated copy of *PcrgA*::$crgA_{MS}$ or *Ptet*::*ecfp*-$crgA_{MT}$ (Fig. 2B; see also Fig. S3B in the supplemental material and compare panels ii to v to panel i). These results suggested two important points. First, the *M. tuberculosis crgA* gene replaced the function of its *M. smegmatis* counterpart. Second, the ECFP-CrgA fusion was functional, and the localization of the fusion protein presumably reflected the native CrgA localization patterns (Fig. 3A). Collectively, these data imply that CrgA plays a role in cell division and cell shape determination in mycobacteria.

CrgA localizes to membranes and septa. The *M. tuberculosis crgA* gene was expressed in *M. smegmatis* as an *ecfp-crgA* fusion from the inducible tetracycline promoter (Table 1), and the localization of the fusion protein was examined by fluorescence microscopy. As expected, the ECFP-CrgA protein showed membrane localization (Fig. 3A). In addition, distinct midcell bands and polar localization were detected (Fig. 3A, panels ii and iv). The midcell localization in some cells was associated with a visible constriction, which suggested that CrgA is a late recruit to the septasomal complex (Fig. 3A, arrows in panel iv). ECFP-CrgA was also present in some cells as spots at midcell or quarter-cell positions (Fig. 3A, panels iv and vi). In dividing cells or those about to split apart, ECFP-CrgA appeared as polar spots, indicating that the protein localized here is either a remnant from midcell division or is engaged in the maturation of cell poles (Fig. 3A, panels i and ii). Distinct septal ring localization was absent in nondividing cells (data not shown). Enumeration of protein localization indicated that 12.9% ± 0.4% of the cells had midcell rings and that 18.0% ± 1.0% of the cells showed polar localization. Midcell and quarter-cell

Downloaded from http://jb.asm.org/ on January 31, 2012 by FLORIDA STATE UNIV

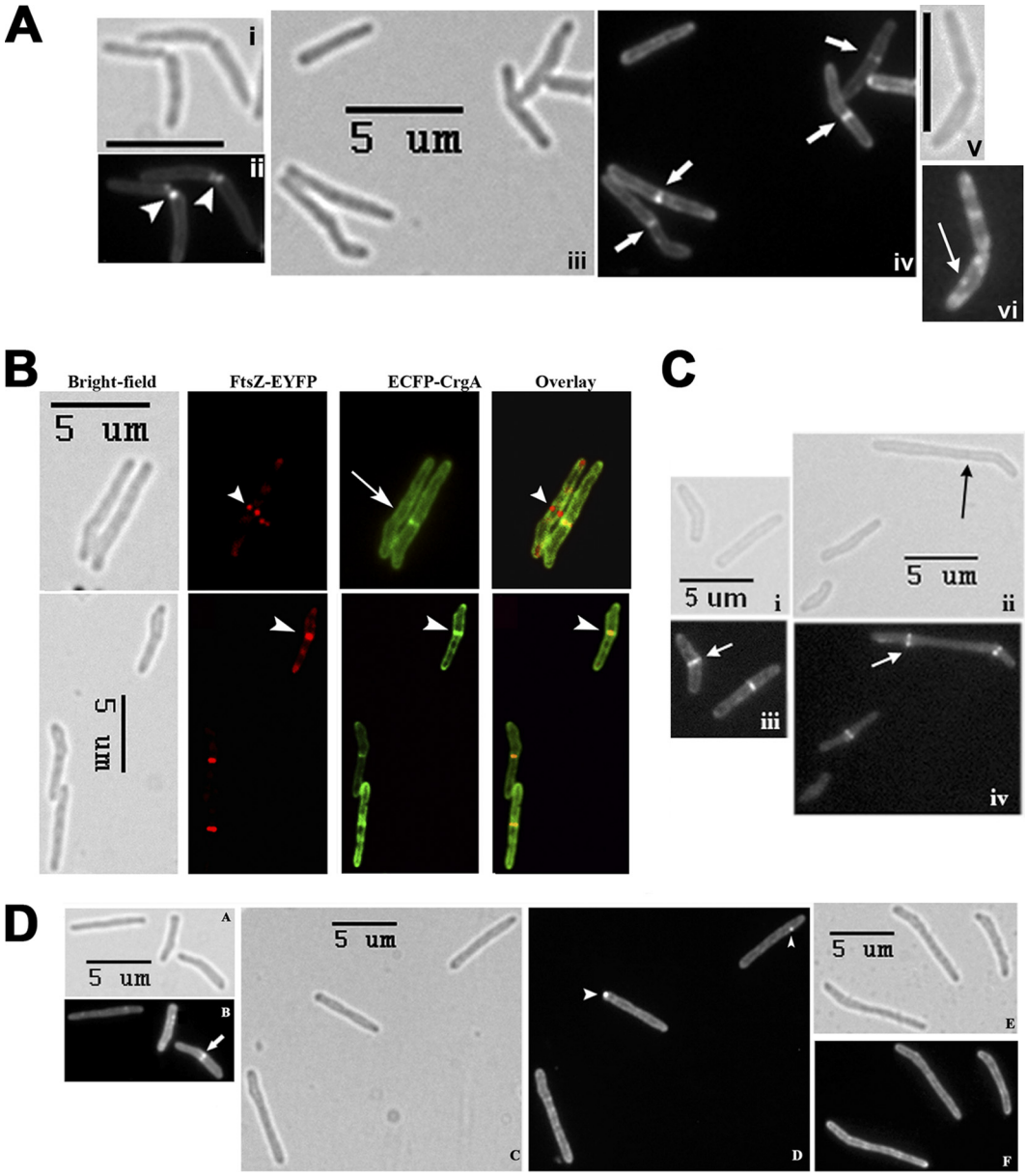

FIG. 3. CFP-CrgA localizes to midcell sites in an FtsZ-dependent manner and colocalizes with FtsZ. (A) An exponential culture of *M. smegmatis Ptet*::*ecfp-crgA* strain was grown with 100 ng/ml anhydrotetracycline for 3 h and examined by bright-field (i, iii, and v) and fluorescence (ii, iv, and vi) microscopy. Arrows represent midcell and spotted localizations, whereas arrowheads indicate localizations at new poles. Bar, 5 μm. (B) *M. smegmatis* strains expressing *Ptet*::*ecfp-crgA* or *Pami*::*ftsZ-eyfp* or both were grown in 7H9-albumin-dextrose broth containing 0.2% acetamide and 100 ng/ml anhydrotetracycline for 3 h. Cells were examined by bright-field and fluorescence microscopy. Images were optimized with Photoshop CS4. Yellow, colocalization; arrowhead, FtsZ-EYFP/ECFP-CrgA colocalization; arrow, absence of ECFP-CrgA from midcell site occupied by FtsZ. (C) FtsZ rings form in the absence of CrgA. Wild-type *M. smegmatis* (i and iii) and a Δ*crgA* strain (ii and iv) expressing *Pami*::*ftsZ-gfp* were grown in broth and imaged by bright-field (i and ii) and fluorescence (iii and iv) microscopy. White arrow, FtsZ-GFP ring; black arrow, unsplit septum. (D) *M. smegmatis* FZ-3 (Δ*ftsZ Pami*::*ftsZ*) *Ptet*::*ecfp-crgA* was grown with 100 ng/ml anhydrotetracycline and without (C to F) or with (A and B) 0.2% acetamide for 3 h and visualized by bright-field (A, C, and E) and fluorescence (B, D, and F) microscopy. Arrow, midcell ECFP-CrgA localization; arrowhead; ECFP-CrgA foci.

foci were present in 15.8% ± 0.6% and 19.6% ± 2.4% cells, respectively. Under these conditions, ECFP-CrgA fusion protein levels were ~2.1-fold greater than the wild-type CrgA levels (data not shown). We did not note any overt changes in growth or cell shape under these conditions. Together, these data suggest that CrgA protein localization is dynamic and possibly shifts from membranes to potential division sites and midcell septa as cell division progresses.

CrgA colocalizes with FtsZ at midcell sites. The septal localization of CrgA prompted us to evaluate whether cells with septal CrgA also have FtsZ at midcell sites. For this purpose, we expressed *Ptet*::*ecfp-crgA* and *Pami*::*ftsZ-eyfp* in *M. smegma-*

Downloaded from http://jb.asm.org/ on January 31, 2012 by FLORIDA STATE UNIV

tis and visualized the fusion proteins by fluorescence microscopy. Induction with 10 ng of anhydrotetracycline and 0.02% acetamide led to ~2.1-fold and 1.8-fold increases in levels, respectively, of ECFP-CrgA and FtsZ-EYFP fusion proteins compared to the respective native protein levels (data not shown) (20). Nearly one-third of the cells (34%; $n = 941$) with midcell FtsZ-EYFP showed colocalization with ECFP-CrgA (Fig. 3B). Furthermore, no cells showed midcell ECFP-CrgA alone (data not shown), whereas many cells showed FtsZ-EYFP (Fig. 3B, arrowhead in the top panel) that did not colocalize with ECFP-CrgA (Fig. 3B, arrow in top panel). Together, these data indicate that CrgA is likely recruited to the septal sites after FtsZ.

FtsZ ring is necessary for the midcell localization of CrgA. To investigate whether the localization of CrgA to the midcell was dependent on the prior localization of FtsZ, we examined ECFP-CrgA localization under conditions where FtsZ was depleted. We expressed *Ptet-ecfp-crgA* from a replicating vector (Table 1) in an FtsZ conditional mutant strain, FZ-3 (*M. smegmatis* Δ*ftsZ Pami*::*ftsZ*) (Table 1) (19). Growth of FZ-3 in the absence of acetamide results in FtsZ depletion and the formation of filaments that eventually lyse (19). When grown in 0.2% acetamide and 100 ng/ml anhydrotetracycline, *M. smegmatis* FZ-3 *Ptet*::*ecfp-crgA* showed a distinct ECFP-CrgA localization to the membrane, midcell sites, and poles, which was similar to the pattern in the wild type (Fig. 3D). However, growth in the absence of acetamide altered CrgA localization. Filamentous cells lacked midcell ECFP-CrgA bands (Fig. 3D, panels C to F) but contained spots along the lateral walls or at the poles in some cases (Fig. 3D, arrowheads). An alteration of FtsZ levels had no effect on CrgA or ECFP-CrgA levels (see Fig. S2, panel ii, in the supplemental material). Together, these data indicated that CrgA localization at midcell septa was perturbed in the absence of FtsZ and suggest that FtsZ is required for the midcell localization of CrgA.

FtsZ rings form in the *crgA* mutant strain. The above data predicted that the absence of CrgA should not impact FtsZ ring assembly. Accordingly, we examined FtsZ-GFP rings in the *crgA* mutant strain expressing *Pami*::*ftsZ-gfp* (Table 1, pJFR79). Using this construct FtsZ-GFP rings can be visualized in *M. smegmatis* without the addition of acetamide, and FtsZ levels increase by ~1.8-fold without any obvious cell division defects (42) (Fig. 3C and data not shown). Distinct FtsZ-GFP rings were present in the mutant strain similar to the wild-type strain (Fig. 3C). Furthermore, FtsZ levels were unaffected in the *crgA* mutant strain (see Fig. S3A in the supplemental material). Together, these data reveal that FtsZ ring assembly or intracellular FtsZ levels in *M. smegmatis* are not dependent on CrgA.

CrgA interacts with FtsZ. Because colocalization of CrgA with FtsZ at midcell septa implied that CrgA directly interacted with FtsZ, we investigated physical interactions between these proteins *in vivo* in a bacterial two-hybrid assay (BACTH) and *in vitro* by pulldown experiments. CrgA showed interactions with itself and with FtsZ in the two-hybrid assay (Fig. 4A). Under the same conditions, CrgA did not interact with ClpX (see Fig. S4A in the supplemental material). Positive results obtained with the T18-CrgA and T25-CrgA fusion proteins indicated that CrgA dimerized or formed higher-order polymers (Fig. 4A). Interactions between CrgA and FtsZ were

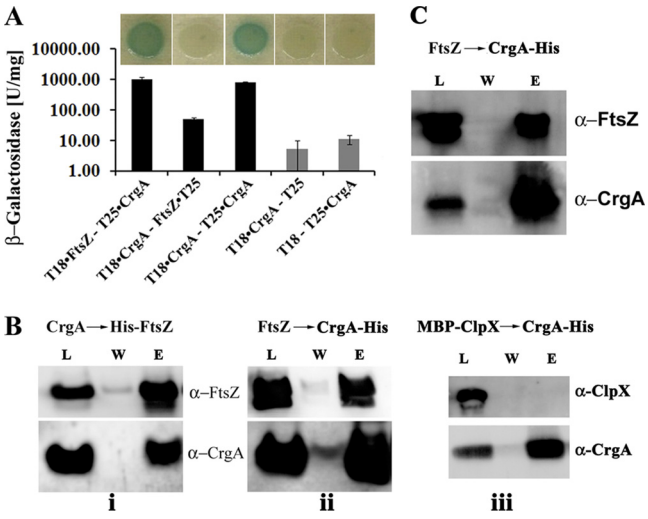

FIG. 4. *M. tuberculosis* CrgA interacts with FtsZ. (A) BACTH assay. CrgA and FtsZ fused to T25 or T18 fragments of the adenylate cyclase in the BACTH vectors (Table 1) were used to transform *E. coli* BTH101 and recombinants plated on LB agar supplemented with X-Gal and IPTG. Green-blue colonies, indicating strong interaction (upper panel), were subsequently grown in broth, and β-galactosidase activity was measured as described in the text. Values are the means ± standard deviations from three independent experiments. (B) Pulldown assay: immunoblots of CrgA pulled down by His-FtsZ (i) and FtsZ pulled down by CrgA-His (ii). Purified CrgA-His (or tag-free CrgA) and tag-free FtsZ (or His-FtsZ) were mixed and loaded onto a cobalt affinity column. Following washing, bound proteins were eluted with imidazole and analyzed by immunoblotting as described in the text. CrgA-His was also mixed with MBP-ClpX and loaded on a cobalt affinity column as a negative control, and fractions were analyzed by immunoblotting (iii). (C) FtsZ and CrgA also interact *in vivo*. Lysates from cells expressing *crgA* and *ftsZ* were mixed together and processed for pulldown on cobalt affinity resin as described for panel B. Load (L), wash (W), and elution (E) fractions are shown. α, anti.

also observed by the pulldown assay as the His-FtsZ retained tag-free CrgA on a cobalt affinity resin column (Fig. 4B, panel i), and, reciprocally, CrgA-His retained tag-free FtsZ (panel ii). Under the same conditions, CrgA-His did not pull down the MBP-ClpX protein (Fig. 4B, panel iii), and pulldown assays with untagged CrgA and FtsZ proteins did not show significant binding of either protein to the resin, which indicated that the interaction between CrgA and FtsZ was specific (see Fig. S4B, panel i, in the supplemental material). The interaction between CrgA-His and FtsZ was also detected using lysates from an *E. coli* strain coexpressing *crgA-his* and tag-free *ftsZ* rather than purified proteins (Fig. 4C).

As the predicted cytoplasmic portion of CrgA consists of a 26-amino-acid N-terminal tail, this region is a likely candidate for direct interaction with FtsZ in the cytoplasm. To test this possibility, we constructed an ECFP-CrgA fusion protein containing the N-terminal 26 amino acids plus the first transmembrane region, i.e., residues 1 to 51 (ECFP-ΔC-term-CrgA). Midcell bands were detected for the ECFP-ΔC-term-CrgA fusion (12.5% ± 0.6%) as previously shown for the full-length fusion, ECFP-CrgA (12.9% ± 0.4%) (see Fig. S5A in the supplemental material). Fusions of CrgA consisting of residues 1 to 25 ($CrgA_{1–25}$) to the N-terminal or C-terminal end of ECFP failed to localize and showed extremely weak and diffuse

Downloaded from http://jb.asm.org/ on January 31, 2012 by FLORIDA STATE UNIV

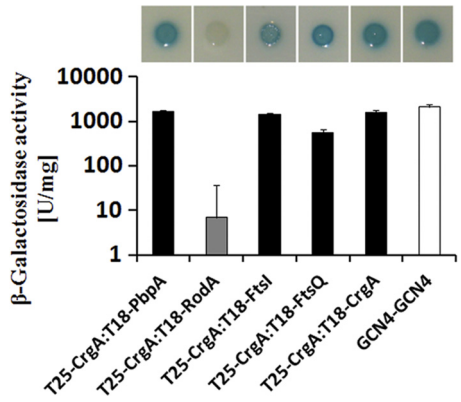

FIG. 5. CrgA interacts with multiple cell division proteins. A BACTH assay was carried out with *crgA*, *pbpA*, *pbpB*, *ftsQ*, *rodA*, and *ftsZ* fused to T25 or T18 fragments of adenylate cyclase as described above (Table 1). GCN4-GCN4 served as a positive control. Means ± standard deviations from three independent experiments are shown.

fluorescence throughout the *M. smegmatis* cell (data not shown). It is likely that either the fusion protein failed to fold properly or that the first transmembrane helix (TMH1) domain imparted stability to the fusion protein. Nevertheless, the N-terminal residues (1 to 51) were sufficient for CrgA localization at the septal sites. BACTH assay revealed that a peptide spanning N-terminal amino acids 1 to 51 also interacted with FtsZ (see Fig. S5B), and the interaction was confirmed by pulldown assay (see Fig. S4B, panel ii).

CrgA interacts with multiple cell division proteins. Next, we examined whether CrgA interacted with the previously identified cell division proteins, FtsI, FtsQ, ClpX, SepF, PBPA, and RodA, using BACTH assays (12, 14, 20, 45). This analysis demonstrated CrgA interactions with FtsI, FtsQ, and PBPA but not with RodA, ClpX, or SepF (Fig. 5; also data not shown). CrgA interactions with PBPA, FtsI, and FtsQ were specific (see Fig. S4A in the supplemental material). BACTH assays with a truncated form of FtsI indicated that the N-terminal 298-amino-acid portion of the protein was sufficient for interaction with CrgA (see Fig. S5B).

Localization of GFP-FtsI and GFP-PBPA. The *M. tuberculosis* FtsI protein was fused to GFP to study its localization in *M. smegmatis* strains that produce different levels of CrgA. At wild-type levels of CrgA, GFP-FtsI localized primarily as midcell and polar foci (Fig. 6A, panel ii). In the *crgA* mutant, the GFP-FtsI localization was diffuse, with weak fluorescence (Fig. 6A, panel iv). In contrast, under CrgA overproduction conditions, distinct midcell GFP-FtsI bands, instead of foci (Fig. 6A, arrowheads in panel vi), with overall increased membrane localization were noted (Fig. 6A, panel vi). When quantitated, 2% of the wild-type cells (n = 213) showed weak midcell bands, whereas 9% of the CrgA-overproducing cells (n = 341) showed vibrant midcell bands. Together, these results indicated that CrgA promotes FtsI localization. Under these experimental conditions, the FtsI and GFP-FtsI levels were comparable in three strains (see Fig. S3A in the supplemental material). We also noted that ~3% of the *ftsI* merodiploid cells with or without *crgA* overexpression were bulged (data not shown).

The GFP-PBPA fusion localized to the membrane and as distinct foci to the poles, quarter-cell, and midcell sites (Fig. 6B, panel ii). The *crgA* mutant strain showed an overall diffuse and nonspecific fluorescence throughout the cell (Fig. 6B, panel iv). However, localization at midcell sites and poles was not significantly affected. These results indicated that the absence of CrgA had only a modest effect on PBPA localization. Distinct midcell GFP-PBPA bands were noted in 3.1% of CrgA-overproducing cells (n = 368) (Fig. 6B, compare panels ii and vi; note arrowheads in panel vi) while no midcell bands were noted in wild-type cells. CrgA overproduction also led to increased membrane localization (Fig. 6B, panel vi).

Localization of penicillin-binding proteins. Labeling of wild-type *M. smegmatis* cells with Bocillin-FL, a fluorescent analog of penicillin, showed distinct foci at midcell and cell poles, which are the potential sites for nascent PG synthesis in mycobacteria (Fig. 6C, panel ii) (6). The Bocillin-FL staining mirrored the GFP-FtsI and GFP-PBPA localization patterns (Fig. 6C, compare WT panels with corresponding panels in A and B). Cells overproducing CrgA exhibited distinct midcell bands and increased membrane staining, whereas the *crgA* mutant cells showed an overall reduced Bocillin-FL staining (Fig. 6C). Together, these data support the conclusion that the CrgA interaction with FtsI and PBPA promotes their recruitment and/or stabilization at the sites of peptidoglycan synthesis.

Muropeptide composition analysis by high-performance liquid chromatography (HPLC) followed by mass spectrometry indicated that CrgA overproduction was not associated with modification of the extent or mode of peptidoglycan cross-linking (see Fig. S6 and Table S1 in the supplemental material).

DISCUSSION

This study focused on Rv0011c, an uncharacterized cell division protein of *M. tuberculosis*. The key findings of our study are the following. First, CrgA, which is encoded by Rv0011c, interacted not only with FtsZ, the initiator of cell division, but also with components of the septasomal assembly and cell wall synthesis, i.e., penicillin-binding proteins, FtsI and PBPA, and FtsQ. Second, the CrgA protein localized to membranes, midcell, and cell poles. Third, the CrgA-FtsI interactions promoted and/or stabilized FtsI assembly at septal sites and on the membrane. While the assembly of FtsZ was not affected by CrgA, the above results are consistent with the notion that CrgA is one of the proteins that is likely involved in a step coordinating Z-ring assembly with the players in cell wall synthesis (see below).

The *Streptomyces* CrgA belongs to a novel family of small proteins involved in sporulation, septation, and developmental differentiation (15, 16). CrgA is required for sporulation septation in *S. avermitilis* but not in *S. coelicolor* although it has been shown to influence the timing of onset of reproductive growth and antibiotic production on glucose-containing medium in the latter species (15, 16). CrgA has been shown to localize to discrete foci, and its overproduction promotes FtsZ proteolytic turnover and thereby inhibits formation of productive cytokinetic rings in *S. coelicolor* (15). On the other hand, a *crgA* deletion is associated with an increase in the abundance of FtsZ rings with premature development of aerial hyphae in

Downloaded from http://jb.asm.org/ on January 31, 2012 by FLORIDA STATE UNIV

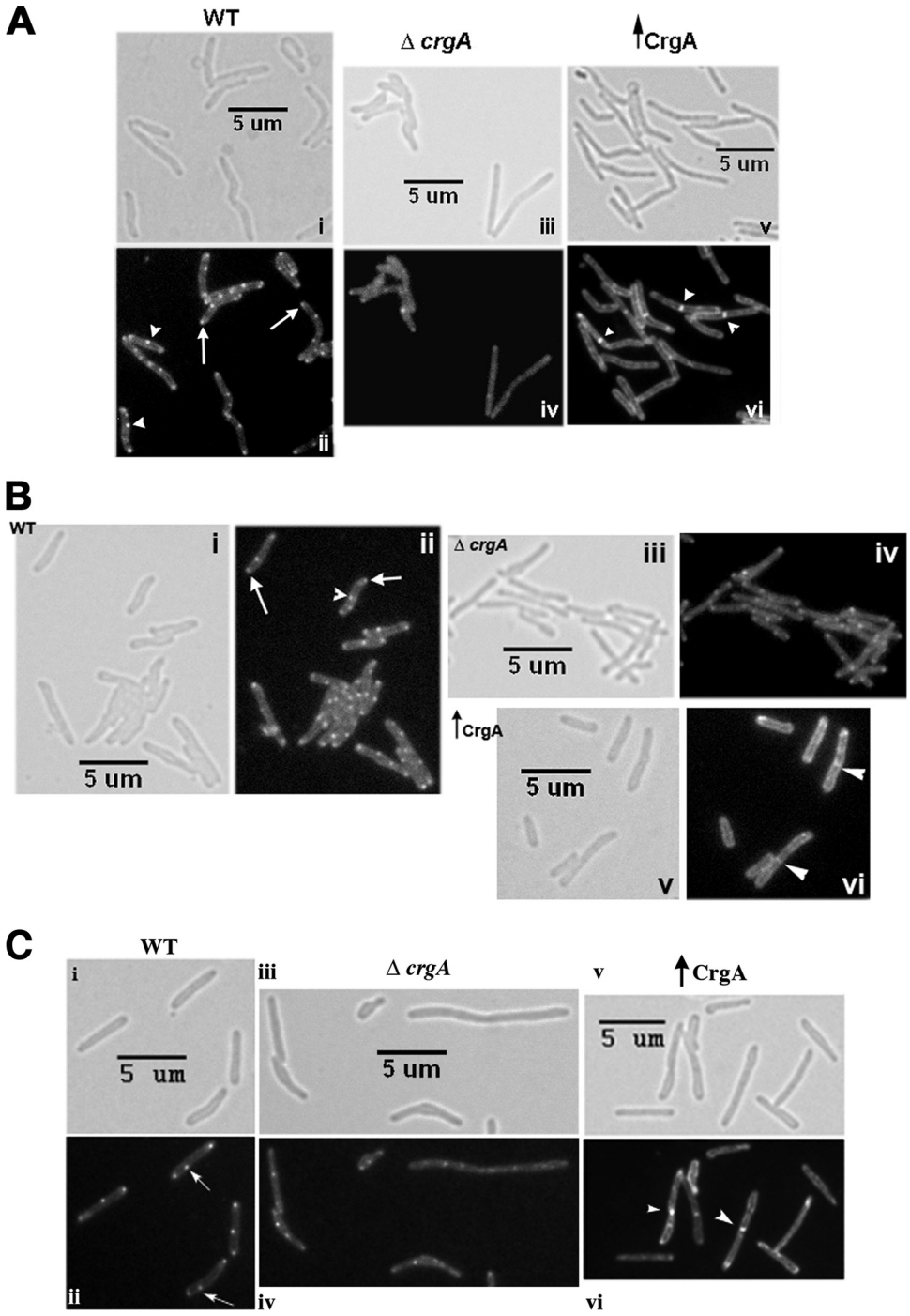

FIG. 6. PBP localization in CrgA strains. (A) GFP-FtsI$_{MT}$ localization. Wild-type (WT), *crgA* mutant (Δ*crgA*), and *crgA* overexpression (↑CrgA) strains of *M. smegmatis Pami*::*gfp-pbpB* were grown with 100 ng/ml anhydrotetracycline and 0.2% acetamide for 5 h, examined by bright-field (top panels) and fluorescence (bottom panels) microscopy, and imaged. (B) GFP-PBPA$_{MT}$ localization. WT, Δ*crgA*, and ↑CrgA strains of *M. smegmatis Pami*::*gfp-pbpA* were grown and imaged as described for panel A by bright-field (i, iii, and v) and fluorescence microscopy (ii, iv. and vi). (C) Bocillin-FL staining. WT, Δ*crgA*, and ↑CrgA *M. smegmatis* strains were grown as described for panel A with 100 ng/ml anhydrotetracycline, stained with Bocillin-FL as described in text, and examined by bright-field (top panels) and fluorescence (bottom panels) microscopy. Midcell and polar localizations are indicated.

S. coelicolor (16). These results implicate *Streptomyces* CrgA in the regulation of FtsZ-ring assembly and possibly sporulation septation. Although *Streptomyces* CrgA shows 74% similarity to CrgA$_{MT}$, the lifestyles of *Streptomyces* spp. and *M. tuberculosis* are different, and our results revealed similarities and significant differences in phenotypes associated with altered levels of CrgA in both organisms. The *M. smegmatis crgA* mutant strain exhibited a swollen cell morphology and ineffi-

Downloaded from http://jb.asm.org/ on January 31, 2012 by FLORIDA STATE UNIV

cient septum splitting, which resulted in a chain-like phenotype. An *S. coelicolor crgA* mutant exhibits a similar, swollen cell phenotype, albeit only in spores and when grown on glucose minimal medium (16). Furthermore, a $CrgA_{MT}$-fluorescent protein fusion localized to discrete foci similar to *Streptomyces* CrgA. However, unlike its *Streptomyces* CrgA counterpart, the ECFP-$CrgA_{MT}$ localized to the membranes as well as to the septa in dividing cells, and $CrgA_{MT}$ overproduction was not associated with any reduction in intracellular FtsZ levels (see Fig. S2, panel i, and S3A in the supplemental material). Furthermore, intracellular *M. smegmatis* FtsZ levels were unaffected, and FtsZ rings remained stable in the *M. smegmatis crgA* mutant. Interestingly, $CrgA_{MT}$ was found to physically interact with FtsZ and other cell division proteins (see below). It is unknown whether *Streptomyces* CrgA behaves in the same manner. Together, these results are consistent with the notion that $CrgA_{MT}$, unlike its *Streptomyces* CrgA counterpart, does not influence Z-ring formation but, rather, could modulate steps subsequent to Z-ring assembly. Thus far, three FtsZ-interacting proteins, FtsW, ClpX, and FipA, have been identified in mycobacteria (13, 20, 45), and CrgA can be added to the list of FtsZ-interacting proteins in mycobacteria.

Our results indicated that CrgA localizes to membranes as well as septa, unlike FtsZ, which localized exclusively to septa. Furthermore, the TMH1 domain of CrgA was required for apparent membrane and septal localization (data not shown; see also Fig. S5A in the supplemental material). Purified CrgA did not bind to *M. smegmatis* peptidoglycans (data not shown), and, therefore, it is likely that CrgA midcell localization is dependent on its interaction with FtsZ. Visualization of CrgA structures in actively dividing cells on membranes and septa suggested that the apparent midcell localization could also result from membrane invagination in dividing cells (Fig. 1B). However, the bright septal localization of CrgA in some cells (Fig. 3A; see also Fig. S5A in the supplemental material) combined with the presence of CrgA foci at midcell and quarter-cell positions ruled out the possibility that the accumulation was due to the joining of two flat cell membranes. Presumably, CrgA localization is dynamic and shifts from membrane to septa, depending on the progress of cell division.

Cell division constitutes two distinct steps: FtsZ-initiated septasome assembly and septum synthesis. While poles and septa are thought to be potential growth zones in mycobacteria, loading of FtsI at the midcell is expected to direct peptidoglycan synthesis at the invaginating septa (17, 37, 53). Thus, it is likely that proteins that interact with FtsI and/or modulate FtsI activity influence peptidoglycan synthesis. We found strong CrgA interactions with FtsQ, PBPA, and FtsI. The latter two proteins are predicted to be transpeptidases involved in peptidoglycan cross-linking during septum synthesis (12, 14). FtsQ is an integral part of the divisome and is believed to play a crucial role in the recruitment of early and late cell division proteins and peptidoglycan polymerases (4, 23, 51). Our studies showed increased GFP-$FtsI_{MT}$ localization at the septa and enhanced Bocillin-FL staining under conditions of CrgA overproduction. This result, combined with the observed strong CrgA interactions with FtsI, PBPA, and FtsQ, supports the notion that CrgA helps to focus peptidoglycan synthesis machinery to the invaginating septa, whereas lack of CrgA delays septal synthesis and splitting, possibly resulting in filamentation. Because CrgA also interacts with FtsZ, this line of thinking leads to an argument that one role of CrgA in mycobacterial cell division is to coordinate FtsZ ring assembly with septum synthesis. CrgA is an abundant protein that is present at ~20,000 molecules per *M. tuberculosis* cell. Because CrgA interacts with several proteins, including the abundant FtsZ protein (~30,000 molecules/cell), it is likely that large amounts of CrgA are required for interactions with multiple proteins. While it is surprising that a small protein like CrgA interacts with multiple cell division proteins, it is not entirely uncommon. *Bacillus subtilis* GpsB is also small protein (98 aa) that interacts with MreC, PBP1, and EzrA (9). Deletion analysis showed that the N-terminal 51 residues of CrgA are sufficient for interaction with FtsZ. It is possible that conserved residues in the transmembrane or extracytoplasmic domain of CrgA are involved in interactions with PBPA and PBPB, the two transpeptidases. Additional work is required to identify the regions and residues involved in interactions with FtsQ, PBPA, and PBP3. Our results also indicated that only the N-terminal region of FtsI is required for interactions with CrgA (see Fig. S5B in the supplemental material). It is pertinent to note that the N-terminal regions of high-molecular-weight PBPs are proposed to mediate protein-protein interactions involved in the assembly of multiprotein complexes (31). Finally, while the CrgA overproduction had similar effects on FtsI and PbpA localization, loss of CrgA had only a marginal effect on PbpA localization but substantially reduced the localization of FtsI. These data together with the cell elongation, bulgy cell, and chain-like phenotype of the *M. smegmatis crgA* mutant suggest a role for CrgA in cell shape and cell wall synthesis processes in mycobacteria.

In *E. coli*, FtsZ and MreB recruit the peptidoglycan synthases for septal and lateral cell wall synthesis (47–49). Mycobacteria lack identifiable homologs for MreB (30). We propose that in the absence of MreB and owing to its interactions with FtsZ, FtsQ, and FtsI, CrgA may facilitate the recruitment of the peptidoglycan synthesis machinery to poles and septal zones and possibly coordinate peptidoglycan synthesis at these sites.

ACKNOWLEDGMENTS

We thank Dorota Stankowska for plasmid pDS5, Renata Dziedzic and Naresh Arora for technical help, and Nabanita Das (Cross lab) and members of the Rajagopalan and Madiraju labs for insightful discussions. We thank Joyoti Basu for antibodies to $FtsI_{MT}$ and S. Ehrt for *Ptet* plasmids.

This work was supported by NIH grants AI48417 (M.R.), AI084734 (M.M.), and AI73891 (T.A.C.).

REFERENCES

1. **Aaron, M., et al.** 2007. The tubulin homologue FtsZ contributes to cell elongation by guiding cell wall precursor synthesis in *Caulobacter crescentus*. Mol. Microbiol. **64:**938–952.
2. **Adams, D. W., and J. Errington.** 2009. Bacterial cell division: assembly, maintenance and disassembly of the Z ring. Nat. Rev. Microbiol. **7:**642–653.
3. **Andrews, J. R., N. S. Shah, N. Gandhi, T. Moll, and G. Friedland.** 2007. Multidrug-resistant and extensively drug-resistant tuberculosis: implications for the HIV epidemic and antiretroviral therapy rollout in South Africa. J. Infect. Dis. **196**(Suppl. 3)**:**S482–S490.
4. **Buddelmeijer, N., and J. Beckwith.** 2004. A complex of the *Escherichia coli* cell division proteins FtsL, FtsB and FtsQ forms independently of its localization to the septal region. Mol. Microbiol. **52:**1315–1327.
5. **Camberg, J. L., J. R. Hoskins, and S. Wickner.** 2009. ClpXP protease degrades the cytoskeletal protein, FtsZ, and modulates FtsZ polymer dynamics. Proc. Natl. Acad. Sci. U. S. A. **106:**10614–10619.

Downloaded from http://jb.asm.org/ on January 31, 2012 by FLORIDA STATE UNIV

6. **Chauhan, A., et al.** 2006. Interference of *Mycobacterium tuberculosis* cell division by Rv2719c, a cell wall hydrolase. Mol. Microbiol. **62:**132–147.
7. **Chauhan, A., et al.** 2006. *Mycobacterium tuberculosis* cells growing in macrophages are filamentous and deficient in FtsZ rings. J. Bacteriol. **188:**1856–1865.
8. **Chung, K. M., H. H. Hsu, H. Y. Yeh, and B. Y. Chang.** 2007. Mechanism of regulation of prokaryotic tubulin-like GTPase FtsZ by membrane protein EzrA. J. Biol. Chem. **282:**14891–14897.
9. **Claessen, D., et al.** 2008. Control of the cell elongation-division cycle by shuttling of PBP1 protein in *Bacillus subtilis*. Mol. Microbiol. **68:**1029–1046.
10. **Corbin, B. D., B. Geissler, M. Sadasivam, and W. Margolin.** 2004. Z-ring-independent interaction between a subdomain of FtsA and late septation proteins as revealed by a polar recruitment assay. J. Bacteriol. **186:**7736–7744.
11. **Dajkovic, A., G. Lan, S. X. Sun, D. Wirtz, and J. Lutkenhaus.** 2008. MinC spatially controls bacterial cytokinesis by antagonizing the scaffolding function of FtsZ. Curr. Biol. **18:**235–244.
12. **Dasgupta, A., P. Datta, M. Kundu, and J. Basu.** 2006. The serine/threonine kinase PknB of *Mycobacterium tuberculosis* phosphorylates PBPA, a penicillin-binding protein required for cell division. Microbiology **152:**493–504.
13. **Datta, P., A. Dasgupta, S. Bhakta, and J. Basu.** 2002. Interaction between FtsZ and FtsW of *Mycobacterium tuberculosis*. J. Biol. Chem. **277:**24983–24987.
14. **Datta, P., et al.** 2006. Interaction between FtsW and penicillin-binding protein 3 (PBP3) directs PBP3 to mid-cell, controls cell septation and mediates the formation of a trimeric complex involving FtsZ, FtsW and PBP3 in mycobacteria. Mol. Microbiol. **62:**1655–1673.
15. **Del Sol, R., J. G. Mullins, N. Grantcharova, K. Flardh, and P. Dyson.** 2006. Influence of CrgA on assembly of the cell division protein FtsZ during development of *Streptomyces coelicolor*. J. Bacteriol. **188:**1540–1550.
16. **Del Sol, R., A. Pitman, P. Herron, and P. Dyson.** 2003. The product of a developmental gene, *crgA*, that coordinates reproductive growth in *Streptomyces* belongs to a novel family of small actinomycete-specific proteins. J. Bacteriol. **185:**6678–6685.
17. **de Pedro, M. A., J. C. Quintela, J. V. Holtje, and H. Schwarz.** 1997. Murein segregation in *Escherichia coli*. J. Bacteriol. **179:**2823–2834.
18. **Dziadek, J., M. V. Madiraju, S. A. Rutherford, M. A. Atkinson, and M. Rajagopalan.** 2002. Physiological consequences associated with overproduction of *Mycobacterium tuberculosis* FtsZ in mycobacterial hosts. Microbiology **148:**961–971.
19. **Dziadek, J., S. A. Rutherford, M. V. Madiraju, M. A. Atkinson, and M. Rajagopalan.** 2003. Conditional expression of *Mycobacterium smegmatis* ftsZ, an essential cell division gene. Microbiology **149:**1593–1603.
20. **Dziedzic, R., et al.** 2010. *Mycobacterium tuberculosis* ClpX interacts with FtsZ and interferes with FtsZ assembly. PLoS One **5:**e11058.
21. **Ebersbach, G., E. Galli, J. Moller-Jensen, J. Lowe, and K. Gerdes.** 2008. Novel coiled-coil cell division factor ZapB stimulates Z ring assembly and cell division. Mol. Microbiol. **68:**720–735.
22. **Fol, M., et al.** 2006. Modulation of *Mycobacterium tuberculosis* proliferation by MtrA, an essential two-component response regulator. Mol. Microbiol. **60:**643–657.
23. **Goehring, N. W., F. Gueiros-Filho, and J. Beckwith.** 2005. Premature targeting of a cell division protein to midcell allows dissection of divisome assembly in *Escherichia coli*. Genes Dev. **19:**127–137.
24. **Gueiros-Filho, F. J., and R. Losick.** 2002. A widely conserved bacterial cell division protein that promotes assembly of the tubulin-like protein FtsZ. Genes Dev. **16:**2544–2556.
25. **Haeusser, D. P., A. H. Lee, R. B. Weart, and P. A. Levin.** 2009. ClpX inhibits FtsZ assembly in a manner that does not require its ATP hydrolysis-dependent chaperone activity. J. Bacteriol. **191:**1986–1991.
26. **Hale, C. A., and P. A. de Boer.** 1999. Recruitment of ZipA to the septal ring of Escherichia coli is dependent on FtsZ and independent of FtsA. J. Bacteriol. **181:**167–176.
27. **Hale, C. A., H. Meinhardt, and P. A. de Boer.** 2001. Dynamic localization cycle of the cell division regulator MinE in *Escherichia coli*. EMBO J. **20:**1563–1572.
28. **Hamoen, L. W., J. C. Meile, W. de Jong, P. Noirot, and J. Errington.** 2006. SepF, a novel FtsZ-interacting protein required for a late step in cell division. Mol. Microbiol. **59:**989–999.
29. **Handler, A. A., J. E. Lim, and R. Losick.** 2008. Peptide inhibitor of cytokinesis during sporulation in *Bacillus subtilis*. Mol. Microbiol. **68:**588–599.
30. **Hett, E. C., and E. J. Rubin.** 2008. Bacterial growth and cell division: a mycobacterial perspective. Microbiol. Mol. Biol. Rev. **72:**126–156.
31. **Holtje, J. V.** 1998. Growth of the stress-bearing and shape-maintaining murein sacculus of *Escherichia coli*. Microbiol. Mol. Biol. Rev. **62:**181–203.
32. **Ishikawa, S., Y. Kawai, K. Hiramatsu, M. Kuwano, and N. Ogasawara.** 2006. A new FtsZ-interacting protein, YlmF, complements the activity of FtsA during progression of cell division in *Bacillus subtilis*. Mol. Microbiol. **60:**1364–1380.
33. **Kang, C. M., S. Nyayapathy, J. Y. Lee, J. W. Suh, and R. N. Husson.** 2008. Wag31, a homologue of the cell division protein DivIVA, regulates growth, morphology and polar cell wall synthesis in mycobacteria. Microbiology **154:**725–735.
34. **Karimova, G., N. Dautin, and D. Ladant.** 2005. Interaction network among *Escherichia coli* membrane proteins involved in cell division as revealed by bacterial two-hybrid analysis. J. Bacteriol. **187:**2233–2243.
35. **Levin, P. A., I. G. Kurtser, and A. D. Grossman.** 1999. Identification and characterization of a negative regulator of FtsZ ring formation in *Bacillus subtilis*. Proc. Natl. Acad. Sci. U. S. A. **96:**9642–9647.
36. **Mukherjee, A., C. Cao, and J. Lutkenhaus.** 1998. Inhibition of FtsZ polymerization by SulA, an inhibitor of septation in *Escherichia coli*. Proc. Natl. Acad. Sci. U. S. A. **95:**2885–2890.
37. **Nanninga, N., F. B. Wientjes, B. L. de Jonge, and C. L. Woldringh.** 1990. Polar cap formation during cell division in *Escherichia coli*. Res. Microbiol. **141:**103–118.
38. **Parish, T., and N. G. Stoker.** 2000. Use of a flexible cassette method to generate a double unmarked *Mycobacterium tuberculosis tlyA plcABC* mutant by gene replacement. Microbiology **146:**1969–1975.
39. **Payne, D. J.** 2008. Microbiology. Desperately seeking new antibiotics. Science **321:**1644–1645.
40. **Pichoff, S., and J. Lutkenhaus.** 2005. Tethering the Z ring to the membrane through a conserved membrane targeting sequence in FtsA. Mol. Microbiol. **55:**1722–1734.
41. **Pichoff, S., and J. Lutkenhaus.** 2002. Unique and overlapping roles for ZipA and FtsA in septal ring assembly in *Escherichia coli*. EMBO J. **21:**685–693.
42. **Rajagopalan, M., et al.** 2005. Genetic evidence that mycobacterial FtsZ and FtsW proteins interact, and colocalize to the division site in *Mycobacterium smegmatis*. FEMS Microbiol. Lett. **250:**9–17.
43. **Stover, C. K., et al.** 1991. New use of BCG for recombinant vaccines. Nature **351:**456–460.
44. **Sugimoto, S., K. Saruwatari, C. Higashi, and K. Sonomoto.** 2008. The proper ratio of GrpE to DnaK is important for protein quality control by the DnaK-DnaJ-GrpE chaperone system and for cell division. Microbiology **154:**1876–1885.
45. **Sureka, K., et al.** 2010. Novel role of phosphorylation-dependent interaction between FtsZ and FipA in mycobacterial cell division. PLoS One **5:**e8590.
46. **Trusca, D., S. Scott, C. Thompson, and D. Bramhill.** 1998. Bacterial SOS checkpoint protein SulA inhibits polymerization of purified FtsZ cell division protein. J. Bacteriol. **180:**3946–3953.
47. **Varma, A., M. A. de Pedro, and K. D. Young.** 2007. FtsZ directs a second mode of peptidoglycan synthesis in *Escherichia coli*. J. Bacteriol. **189:**5692–5704.
48. **Varma, A., and K. D. Young.** 2009. In *Escherichia coli*, MreB and FtsZ direct the synthesis of lateral cell wall via independent pathways that require PBP 2. J. Bacteriol. **191:**3526–3533.
49. **Vats, P., Y. L. Shih, and L. Rothfield.** 2009. Assembly of the MreB-associated cytoskeletal ring of *Escherichia coli*. Mol. Microbiol. **72:**170–182.
50. **Weart, R. B., S. Nakano, B. E. Lane, P. Zuber, and P. A. Levin.** 2005. The ClpX chaperone modulates assembly of the tubulin-like protein FtsZ. Mol. Microbiol. **57:**238–249.
51. **Weiss, D. S., J. C. Chen, J. M. Ghigo, D. Boyd, and J. Beckwith.** 1999. Localization of FtsI (PBP3) to the septal ring requires its membrane anchor, the Z ring, FtsA, FtsQ, and FtsL. J. Bacteriol. **181:**508–520.
52. **White, E. L., et al.** 2000. Slow polymerization of *Mycobacterium tuberculosis* FtsZ. J. Bacteriol. **182:**4028–4034.
53. **Woldringh, C., P. G. Huls, E. Pas, G. J. Brakenhoff, and N. Nanninga.** 1987. Topography of peptidoglycan synthesis during elongation and polar cap formation in a cell division mutant of *Escherichia coli*. J. Gen. Microbiol. **133:**575–586.

Downloaded from http://jb.asm.org/ on January 31, 2012 by FLORIDA STATE UNIV